Design of an Integrated Bragg-Assisted Tunable Silicon Microring for Orbital Angular Momentum Generation

Fabrizio Gambini[1,2,3], *Student Member, OSA*, Philippe Velha[1], *Member, OSA*, Jonathan Klamkin[3], *Senior Member, OSA*, and Stefano Faralli[1]

[1] *Scuola Superiore Sant'Anna, via G. Moruzzi 1, 56124, Pisa, Italy*
[1] *CNIT Photonic Networks National Laboratory, via G. Moruzzi 1, 56124, Pisa, Italy*
[3] *Electrical and Computer Engineering Department, University of California, Santa Barbara, CA 93106*
fabrizio.gambini@sssup.it

Abstract: An integrated tunable $10-\mu m$ radius ring resonator assisted by silica holes for orbital angular momentum (OAM) generation is designed exploiting an integrated heater enabling the generation of different OAM states at the same wavelength.

OCIS codes: (130.0130) Integrated optics, (130.3120) Integrated optics devices.

1. Introduction

Helical phase fronts can support orbital angular momentum (OAM) equal to $l \cdot \hbar$ per photon, where l is the topological charge and $\hbar$ is the reduced Planck constant [1]. The mutual orthogonality, the reduced cross-talk [2] and the theoretical infinite number of OAM states supported for the single light beam [3] can be exploited to increase the spectral efficiency of optical communication systems, providing an additional dimension of data carriers in space division multiplexing and mode division multiplexing systems, which could benefit free space optical communications. For these reasons, many efforts have been carried out recently to design and demonstrate low power consumption and high efficiency OAM emitter solutions. Silicon photonics in particular provides a path toward large-scale integration. In [4], a passive ring resonator with internal sidewall gratings for azimuthally-polarized optical vortex emission was proposed and demonstrated. A version with thermo-optic heaters was manufactured to switch between OAM modes [5]. Although the thermal efficiency is high, a thin silicon dioxide layer ($300\,nm$ is needed [4]) introducing a fabrication constraint. Here, based on [6], we propose, with the support of finite-difference time domain (FDTD) [7] and finite-element method (FEM) [8] simulations, a small footprint thermally tunable ring resonator for a radially-polarized OAM emitter. The study relaxes the fabrication constraints for silicon-on-insulator (SOI) platforms. Furthermore, the losses for both propagating and emitted optical fields are reduced. [1]

2. Device design

The emitter comprises a single $10-\mu m$ radius ring resonator with a single mode transverse-electric (TE) $500-nm$ wide, $220-nm$ tall silicon waveguide, with q equidistant fully-etched holes along the central path with a diameter of $100\,nm$. The holes are filled with silica. The bus waveguide is bent by an angle α to increase the coupling coefficient in order to achieve the critical coupling condition. The integrated ring resonator is reported in Fig. 1(a). The effective index of the fundamental mode is $n_{eff} = 2.422150$ and in Fig. 2 the distribution of the transverse (a) and azimuthal (b) polarization components (in the presence of the silica-filled hole) of the electric field are reported, demonstrating that the former is concentrated in the center of the waveguide. The silica holes allow for the scattering of the radial electrical field polarization, enabling the coupling of the whispering gallery modes (WGM) to OAM modes. Furthermore, the scattering of this component increases the ring loss with an increment of the bandwidth, while reaching high emission efficiency, low back-reflection, and small device footprint.

The order l of a radiated OAM mode is [4]:

$$l = p - g \cdot q = p - q \tag{1}$$

where g is the integer diffraction order ($g = 1$ in this study) and p is the order of the WGM mode propagating in the ring resonator, and is related to the resonant wavelength λ_{res} and n_{eff} through:

[1] This work is partially supported by the Italian Ministry of Education, University and Research (MIUR) through the FIRB project MINOS, by the Italian Ministry of Foreign Affairs (MAE-UST) through the high-relevance bilateral project NANO-RODIN, by Scuola Superiore SantAnna and by the European Commission through the FP7 project IRIS (no. 619194). The authors would like also to acknowledge Dr. C. J. Oton and Dr. P. Pintus for their help and valuable discussions.

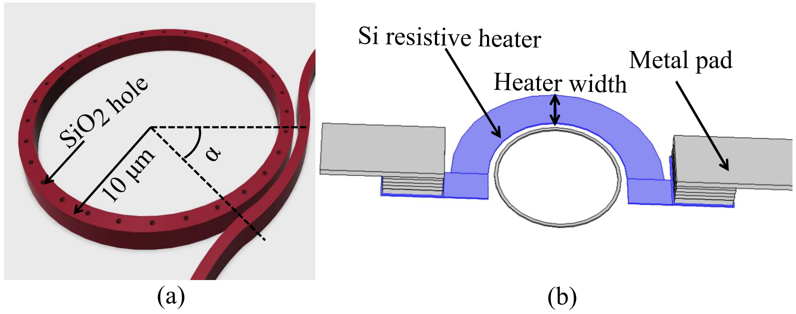

Fig. 1. OAM emitter top-view (a) and integrated heater schematic (b).

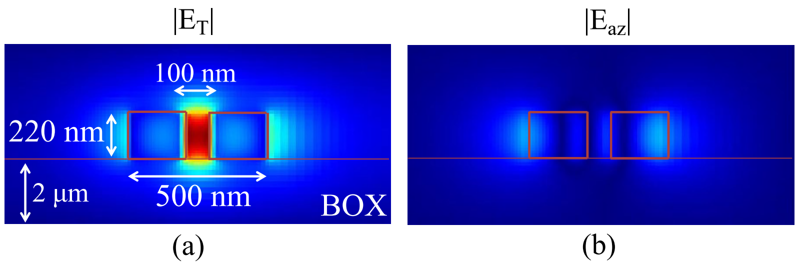

Fig. 2. Transverse (a) and azimuthal (b) polarization components of the propagating electric field in the microring resonator.

$$p = \frac{L_g \cdot n_{eff}}{\lambda_{res}} \Leftrightarrow l = \frac{L_g \cdot n_{eff}}{\lambda_{res}} - q \tag{2}$$

where L_g is the geometrical resonating length, and therefore for a fixed λ_{res}, the order l can be modulated by varying the value of n_{eff}. In this work, the integer $q = 98$ has been set in order to achieve $l = 0$ near $1550\,nm$.

From the simulation results, the free-spectral range (FSR) is $9.55\,nm$ and the calculated group index (n_g) is 3.9. By applying equation (3), which relates the resonance wavelength shift and the temperature variation, a complete FSR shift is obtained for a temperature variation equal to $127\,K$.

$$\frac{\Delta\lambda}{\lambda} = \frac{1}{n_g}\frac{\partial n_{eff}}{\partial n_{core}}\frac{\partial n_{core}}{\partial T}\Delta T + \frac{1}{n_g}\frac{\partial n_{eff}}{\partial n_{clad}}\frac{\partial n_{clad}}{\partial T}\Delta T \Rightarrow \Delta\lambda = 0.0743\Delta T \tag{3}$$

where the effective index variations have been calculated from the modal analysis, and the material temperature dependence can be found in [9]. A study on an integrated heater aiming to maximize the tuning efficiency while reducing the optical loss is proposed. The thermal analysis has been developed through multiphysics simulations. The schematic of the heater is reported in Fig. 1(b). The conductive path that surrounds the emitter is composed of highly doped phosphorous-implanted silicon (n++, electron carrier density of $1e^{20}$). The n++ silicon height ($220\,nm$) and the distance from heater to ring waveguide ($1\,\mu m$) allow for maximizing the tuning efficiency and minimizing the optical loss. The width of the conductive path ($9\,\mu m$) corresponding to a resistance of approximately $1.445\,k\Omega$ reduces the electrical power consumption; the IV characteristic is reported in the top of Fig. 3(a). The bottom of the same figure shows the dependence of temperature variation on dissipated power. A temperature variation of $127\,K$ corresponds to a total dissipated power of approximately $95\,mW$. Also, the $1-\mu m$ wide silica layer provides thermal isolation and improves the thermal tuning efficiency.

In Fig. 3 (b) the response calculated at the through port is shown with the corresponding expected OAM patterns in the insets. Due to space constraints, here only right-handed circularly polarized (RHCP) beams are reported with $l+1$ spiral arms [6]. The same result is obtained in (c). While applying a temperature variation of $\Delta T = 127\,K$ (equal to a shift of the wavelength response equal to a FSR) and $\Delta T = 254\,K$ (equal to two FSR), in (d) and (e) respectively, it is demonstrated that the device supports OAM states.

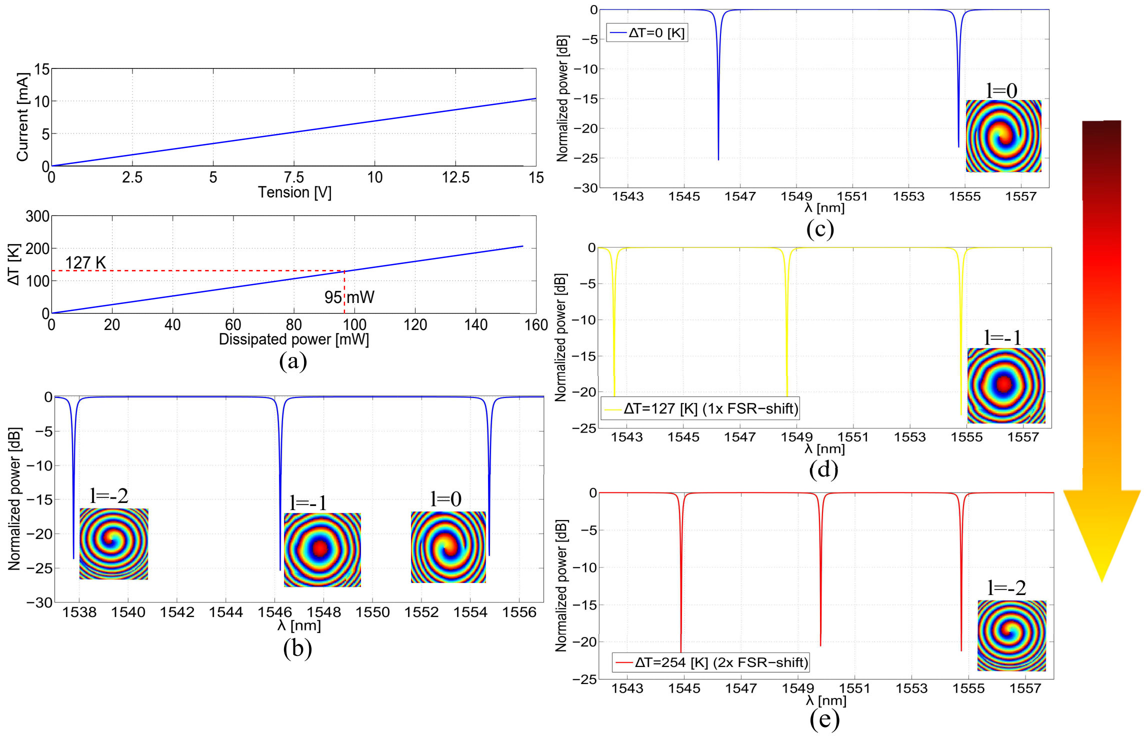

Fig. 3. Current vs. tension and temperature variation vs. dissipated power characteristics (a), ring resonator spectrum at the output of the bus and the related expected RHCP vortexes for different topological charge (b), resonance shift and expected OAM RHCP mode at $1555\,nm$ for different temperature variations: $\Delta T = 0\,K$ (a), $\Delta T = 127\,K$ equal to a FSR-shift (b) and $\Delta T = 254\,K$ equal to two FSR-shift (c).

3. Conclusion

The design of an integrated tunable OAM emitter has been proposed allowing for switching between OAM mode order. The performance evaluation shows a minimum dissipated power of $95\,mW$ for a complete FSR shift. The design mitigates optical loss and fabrication constraints enabling the access to OAM mode multiplexing at the same resonating wavelength.

References

1. Allen L. *et al.*, "Orbital angular momentum of light and the transformation of Laguerre-Gaussian laser modes," Phys. Rev. A vol. 45, no. 11, pp. 8185-81809, Jun. 1992
2. A. E. Willner *et al.*, "Optical communications using orbital angular momentum beams," Adv. Opt. Photon., vol. 7, pp. 66-106, Mar. 2015
3. B. Guan, *et al.*, "Free-space coherent optical communication with orbital angular, momentum multiplexing/demultiplexing using a hybrid 3D photonic integrated circuit," Opt. Express, vol. 22, pp. 145-156, Jan. 2014
4. X.Cai *et al.*, "Integrated Compact Optical Vortex Beam Emitters," Science, vol. 338, no. 6105, pp. 363-366, Oct. 2012
5. M. J. Strain *et al.*, "Fast electrical switching of orbital angular momentum modes using ultra-compact integrated vortex emitters," Nat. Commun., vol. 5, no. 4856, Sept. 2014
6. F. Gambini *et al.*, "Demonstration of an Ultra-Compact Photonic Integrated Orbital Angular Momentum Emitter with a Bragg Grating Silicon Microring," in Proc. Optical Fiber Communications (OFC) conference (2016), paper Th3E.3.
7. Lumerical Solutions, Inc., Innovative Photonic Design Tools, www.lumerical.com
8. COMSOL Multiphysics, www.comsol.com
9. L. Chrostowski, and M. Hochberg, "Silicon Photonics Design: From Devices to Systems," (2015).